

Mononuclear, Dinuclear and Polymeric Complexes of Cu(II) with Polypyridyl Ligands: Synthesis, Characterization, Crystal Structure, Interaction with DNA and BSA, and *In-Vitro* Anticancer Activity

Khatereh Abdi

k.abdi@ch.iut.ac.ir

September 14, 2014

Department of Chemistry, Isfahan University of Technology, 84156-83111, Isfahan, Iran

1st Supervisor: Prof. H. Hadadzadeh*, hadad@cc.iut.ac.ir

2nd Supervisor: Dr. M. Salimi**, salimimona@pasteur.ac.ir

Advisor: Prof. S. Mallakpour*

Department Graduate Coordinator: Dr. A.R. Najafi

* Isfahan University of Technology, 84156-83111, Isfahan, Iran

** Department of Physiology and Pharmacology, Pasteur Institute of Iran, Tehran, P.O. Box 13164, Iran

Abstract

In this thesis, four new polypyridyl complexes of Cu(II) with formulation $[\text{Cu}(\text{tptz})(\text{dppz})](\text{PF}_6)_2$, $[\text{Cu}(\text{tpy})(\text{dppz})](\text{PF}_6)_2$, $[\{\text{Cu}(\text{tppz})\text{Cl}\}_2(\mu\text{-Cl})](\text{PF}_6)_2 \cdot \text{toluene}$, and $[\text{Cu}_2(\mu\text{-Cl})_2(\mu\text{-tppz})]_n(\text{PF}_6)_{2n}$ (where tptz = 2,4,6-tris(2-pyridyl)-1,3,5-triazine, dppz = dipyrido[3,2-*a*:2',3'-*c*]phenazine, tpy = 2,2':6',2''-terpyridine, and tppz = 2,3,5,6-tetrakis(2-pyridyl)pyrazine) were synthesized and characterized. Furthermore, two other Cu(II) complexes, $[\text{Cu}(\text{tptz})\text{Cl}_2] \cdot 2\text{H}_2\text{O}$ and $[\text{Cu}(\text{tptz})_2](\text{PF}_6)_2$, were considered for complementary studies such as the determination of crystal structure and biological activities. The solid state structures of $[\text{Cu}(\text{tptz})\text{Cl}_2] \cdot 2\text{H}_2\text{O}$, $[\text{Cu}(\text{tpy})(\text{dppz})](\text{PF}_6)_2$, $[\{\text{Cu}(\text{tppz})\text{Cl}\}_2(\mu\text{-Cl})](\text{PF}_6)_2 \cdot \text{toluene}$, and $[\text{Cu}_2(\mu\text{-Cl})_2(\mu\text{-tppz})]_n(\text{PF}_6)_{2n}$ were determined by single-crystal X-ray crystallography. Several biological activities of $[\text{Cu}(\text{tptz})_2](\text{NO}_3)_2$, $[\text{Cu}(\text{tptz})(\text{dppz})](\text{NO}_3)_2$, $[\text{Cu}(\text{tpy})(\text{dppz})](\text{ClO}_4)_2$, and $[\{\text{Cu}(\text{tppz})\text{Cl}\}_2(\mu\text{-Cl})](\text{NO}_3)_2$ were investigated. The mode and propensity for the binding of these complexes to DNA were studied by different spectroscopic, voltammetric, and gel electrophoresis techniques. The results show that $[\text{Cu}(\text{tptz})(\text{dppz})](\text{NO}_3)_2$ and $[\text{Cu}(\text{tpy})(\text{dppz})](\text{ClO}_4)_2$ are avid metalointercalators to DNA. The nuclease activity of $[\text{Cu}(\text{tptz})_2](\text{NO}_3)_2$, $[\text{Cu}(\text{tpy})(\text{dppz})](\text{ClO}_4)_2$, and $[\{\text{Cu}(\text{tppz})\text{Cl}\}_2(\mu\text{-Cl})](\text{NO}_3)_2$ was also examined by agarose gel electrophoresis. Moreover, the *in-vitro* anticancer activity of these three complexes on the human breast adenocarcinoma (MCF-7) cell line was evaluated by an MTT assay. The results indicate that these complexes (specially $[\text{Cu}(\text{tptz})_2](\text{NO}_3)_2$ and $[\text{Cu}(\text{tpy})(\text{dppz})](\text{ClO}_4)_2$) have marked cell growth-inhibitory effects with the IC_{50} values which are significantly better than that observed for *cis*-platin under the same experimental conditions. In addition, the apoptotic activity of $[\text{Cu}(\text{tptz})_2](\text{NO}_3)_2$ and $[\text{Cu}(\text{tpy})(\text{dppz})](\text{ClO}_4)_2$ on MCF-7 cells was assessed *via* DAPI staining. The interaction of $[\{\text{Cu}(\text{tppz})\text{Cl}\}_2(\mu\text{-Cl})](\text{NO}_3)_2$ with BSA was monitored using fluorescence and electronic absorption spectroscopies.

Key Words

Cu(II) polypyridyl complexes, X-ray crystallography, DNA interaction, BSA interaction, Linear dichroism spectroscopy, Nuclease activity, Cytotoxicity.

Introduction

Metal-based pharmaceuticals emerging from interface of inorganic chemistry, pharmacology, toxicology and biochemistry have witnessed spectacular successes (Chauhan, 2007). The discovery of the cytotoxic properties of *cis*-platin provided enormous impetus for research into the use of metal complexes in the fight against cancer. This search is aided by the application of numerous techniques from the toolbox of the inorganic chemist, particularly knowledge of the coordination behavior, photophysical,

photochemical and redox properties of metal complexes (Zhang and Lippard, 2003).

Design of metal-based pharmaceuticals depends on the ligand framework, the choice of metal ion, and its oxidation state. As the biological activity of a complex depends strongly on the nature of the ligands and the coordination behavior of the metal, recent researches have been directed at the synthesis and evaluation of the biological activity of metal complexes with biologically interesting ligands with the aim of widening the spectrum of complex activity. A combination of the activity of the metal and the activity of its organic ligands may reveal new modes of action (Chauhan, 2007; Patel et al., 2012).

One active area of interest in bioinorganic chemistry is the design and characterization of transition metal complexes with polypyridyl ligands because of their interesting photophysical, photochemical and electronic properties, diverse chemical reactivity, possible use as light sensitive probes in biological systems and unusual structures, which result in noncovalent interactions with DNA (Chen et al., 2011; Barve et al., 2009). The literature reveals that polypyridyl complexes display sequence specific binding, so one can hope to achieve selective binding of a mutated DNA sequence in cancer cells compared to untransformed cells, thereby decreasing the unwanted toxicity of the chemotherapeutics. Furthermore, as drug efflux is believed to be an important contributing factor in *cis*-platin resistance, polypyridyl ligands, due to their stronger DNA binding capacity, may decrease resistance via cellular efflux (Palanichamy et al., 2012).

Amongst the first row transition metal complexes, copper complexes have been widely used as DNA foot printing agents, as structural probes for DNA, and as potential anticancer drugs, since the discovery of first chemical nuclease, $[\text{Cu}(\text{phen})_2]^+$, by Sigman et al. in 1979 (Song et al., 2008). Copper is a bioessential element in all living systems in appropriate oxidation states and it may be less toxic than non-essential metals such as platinum (Chen et al., 2011). It has been demonstrated that copper accumulates in tumors due to the selective permeability of cancer cell membranes to copper compounds (Chen et al., 2010). Because of this biological relevance, a large number of copper(II) complexes have been synthesized and screened for anticancer activity, and some of them were found to be active both *in-vitro* and *in-vivo* (Santini et al., 2013).

Herein, we described the synthetic, spectral and structural-features of several copper(II) complexes with polypyridyl ligands, as well as examining some of their biological activities such as DNA binding, BSA binding, nuclease activity, *in-vitro* cytotoxicity, and apoptotic activity.

Methods

Synthesis of $[\text{Cu}(\text{tptz})(\text{dppz})](\text{PF}_6)_2$

A suspension of $[\text{Cu}(\text{tptz})\text{Cl}_2] \cdot 2\text{H}_2\text{O}$ (96.6 mg, 0.20 mmol) in EtOH (25 mL) was treated with AgNO_3 (68.0 mg, 0.40 mmol) in the dark, while being stirred continuously at room temperature for 1 h. The resulting mixture was cooled to -5°C overnight and filtered through Celite to remove the fine white AgCl precipitate. To the filtrate was then added 1,10-phenanthroline-5,6-dione (phen-dione, 42.0 mg, 0.20 mmol) and the reaction mixture was stirred at room temperature for 2 h. The green precipitate was collected on a fine frit and washed with cold EtOH and diethyl ether. Then the green solid was dissolved in a minimum amount of water and precipitated from solution as the hexafluorophosphate salt by addition of an excess amount of NH_4PF_6 . The product, $[\text{Cu}(\text{tptz})(\text{phen-dione})](\text{PF}_6)_2$, was collected by suction filtration.

1,2-Diaminobenzene (16.2 mg, 0.15 mmol) was added at room temperature with stirring to a solution of the phen-dione complex, $[\text{Cu}(\text{tptz})(\text{phen-dione})](\text{PF}_6)_2$, (87.6 mg, 0.10 mmol) in CH_3CN (1 mL) containing one drop of glacial acetic acid in a small screw-

capped vial. After 10 min, the crude product was precipitated by adding 5 mL of a 10% aqueous solution of ammonium hexafluorophosphate, collected on a filter and rinsed successively with cold water and diethyl ether, and then air dried. For further purification, the green precipitate was recrystallized by slow diffusion of diethyl ether into a solution of the complex in CH₃CN.

Synthesis of [Cu(tpy)(dppz)](PF₆)₂

The complex was prepared by adding 1,2-diaminobenzene (16.0 mg, 0.15 mmol) at room temperature with stirring to a solution of the starting complex, [Cu(tpy)(phen-dione)](PF₆)₂·CH₃CN, (84.0 mg, 0.10 mmol), in CH₃CN (1 mL) containing one drop of glacial acetic acid. After 10 min, the crude product was precipitated by adding 5 mL of a 10% aqueous solution of NH₄PF₆, collected on a filter and washed successively with cold water and diethylether and then air dried. For further purification, the blue-green microcrystalline precipitate was recrystallized by slow diffusion of diethylether into a saturated solution of the complex in CH₃CN/MeOH (1:2).

Synthesis of [{Cu(tppz)Cl}₂(μ-Cl)](PF₆)·toluene

A solution of tppz (155.4 mg, 0.400 mmol) in DMF (10 mL) was added dropwise to a solution of CuCl₂·2H₂O (68.2 mg, 0.40 mmol) in DMF (10 mL) with constant vigorous stirring at room temperature for 3 h. A solution of AgPF₆ (50.6 mg, 0.20 mmol) was then added to the reaction mixture in the dark, while being stirred continuously at room temperature for 2 h. The green solution was evaporated to dryness. Recrystallization was achieved by slow evaporation of a 3:2 methanol/toluene solution of the complex.

Synthesis of [Cu₂(μ-Cl)₂(μ-tppz)]_n(PF₆)_{2n}

A solution of CuCl₂·2H₂O (68.2 mg, 0.40 mmol) and tppz (77.7 mg, 0.20 mmol) in 30 mL DMF was refluxed for 12 h. Then a solution of AgPF₆ (101.1 mg, 0.400 mmol) in 5 mL DMF was then added to the reaction mixture in the dark and refluxed for a further 3 h. The resulting mixture was cooled to -5 °C overnight and filtered through Celite to remove the fine white AgCl precipitate. The green solution was evaporated to dryness. Recrystallization was achieved by slow diffusion of diethylether into a saturated solution of the complex in CH₃CN/MeOH (3:1).

X-ray crystallographic procedures

X-ray diffraction measurements were performed on a Bruker APEXII four-circle diffractometer equipped with a CCD camera, using Mo-Kα radiation ($\lambda = 0.71073$ Å). The data were corrected for absorption using the semi-empirical multiscan approach (SADABS). The structures were solved by direct methods using SHELXS97 and subsequent Fourier analyses and refined by the full-matrix least-squares method using SHELXL97, based on F^2 with all reflections. All non-hydrogen atoms were refined anisotropically.

General procedure for DNA binding studies

For biological studies, the hexafluorophosphate salt of the complexes was converted to its nitrate or perchlorate salt. The purity and concentration of DNA solution was determined spectrophotometrically. The mode and propensity for the binding of the complexes to DNA were studied by different experimental techniques such as electronic absorption, fluorescence, circular dichroism, flow linear dichroism, cyclic voltammetry, differential pulse voltammetry, and gel electrophoresis mobility shift assay. For each

experiment, the mixed complex–DNA solution was allowed to equilibrate for appropriate time.

General procedure for BSA binding studies

The BSA binding studies were performed by electronic absorption and fluorescence spectroscopies. The concentration of BSA solution was determined based on its molecular weight of 66000 Da. The absorption titration experiments were carried out by keeping the concentration of BSA constant while varying the concentration of complex. The absorbance values were recorded after each successive addition of BSA solution and equilibration. The fluorescence titration experiments were performed at a fixed BSA concentration. After incubation time, sample was excited at 290 nm and the emission was recorded between 300 and 500 nm.

DNA cleavage and mechanism study

The DNA cleavage experiments were performed by agarose gel electrophoresis as follows: pEGFP-N1 DNA (100 ng/ μ L) was treated with the complex at various concentrations (5–200 μ M) in the absence and presence of external agents. The samples were incubated for 3 h at 37 °C (or at room temperature), and then electrophoresed on a 0.7% agarose gel using TBE buffer. The bands were then visualized by the UV light and photographed. Furthermore, to obtain information about the reactive oxygen species (ROS) which were responsible for the DNA damage, the nuclease activity of the complex was investigated in the presence of various radical scavengers such as NaN₃ (singlet oxygen quencher), DMSO (hydroxyl radical scavenger) and SOD (superoxide dismutase, superoxide scavenger).

Cell culture and MTT assay

Human breast adenocarcinoma cell line (MCF-7) was obtained from the cell bank of Pasture Institute of Iran, and routinely cultured in RPMI 1640 medium supplemented with 10% (v/v) FBS, 2 mM glutamine, 100 U/mL penicillin and 100 μ g/mL of streptomycin under the conditions of 5% CO₂ at 37 °C. The cytotoxicity was determined by the 3-(4,5-dimethylthiazol-2-yl)-2,5-diphenyltetrazolium bromide (MTT) assay. The MCF-7 cells (8×10^3 cells/well) were cultured in 96-well plates. After incubation overnight, the cell culture medium in each well was replaced by different concentrations (0.01–100 μ M) of the complex and further incubated for appropriate time (24, 48 and 72 h). Afterwards, 20 μ L of MTT (5 mg/mL in PBS) was added to each well and the cells were incubated for another 4 h at 37 °C. The supernatants were then aspirated carefully and 200 μ L of DMSO was added to each well. The plates were shaken for an additional 15 min and the absorbance values were read by the Microplate Reader at 545 nm.

DAPI staining

The MCF-7 cells were incubated with the complex at its IC₅₀ concentration for 16 h. The treated and negative-control cells were stained by DAPI (Diamidine phenyl dihydrochloride) and their morphology was observed under a Zeiss Fluorescence microscope and the photomicrographs were taken with an Olympus digital camera.

Results and Discussion

The [Cu(tptz)Cl₂] \cdot 2H₂O complex

An ORTEP view of the [Cu(tptz)Cl₂] \cdot 2H₂O complex is shown in Figure 1. The asymmetric unit of this complex is built up of one discrete neutral [Cu(tptz)Cl₂] and two

water solvent molecules in which the tptz ligand functions as a tridentate ligand and coordinates through its major coordination sites, involving one triazine and two adjacent pyridyl nitrogen atoms. The coordination geometry of Cu(II) is completed by two chloride anions. Using Addison's model, the angular structural index parameter (τ) for this complex was determined to be 0.116. Thus, the CuN_3Cl_2 coordination polyhedron around the copper(II) center is best described as nearly square-pyramidal.

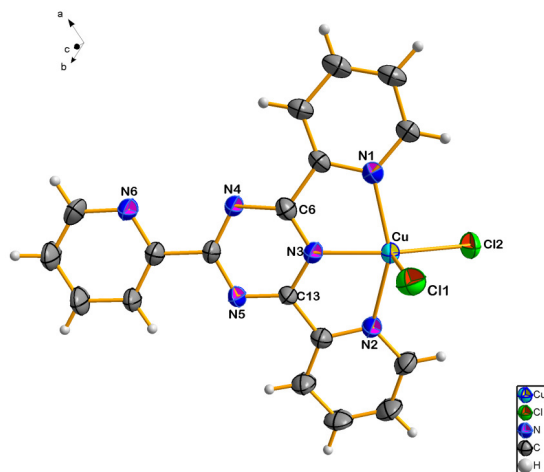


Figure 1. ORTEP view of the molecular structure of $[\text{Cu}(\text{tptz})\text{Cl}_2] \cdot 2\text{H}_2\text{O}$.

The $[\text{Cu}(\text{tptz})_2](\text{PF}_6)_2$ complex

The $[\text{Cu}(\text{tptz})_2](\text{NO}_3)_2$ complex was considered for some biological activities such as DNA binding, nuclease activity, *in-vitro* cytotoxicity and apoptotic activity on MCF-7. The interaction of the complex with DNA has been investigated by electronic absorption, competitive fluorescence titration (EthBr displacement assay), voltammetric techniques and gel electrophoresis mobility shift assay. Based on the following results, it can be concluded that the complex binds to DNA *via* partial intercalation and/or groove binding:

- 1) A moderate hypochromism along with no apparent bathochromism in the UV absorptions of the Cu(II) complex upon increasing the amount of FS-DNA (Figure 2A).
- 2) The fluorescence intensity of EthBr bound to FS-DNA is quenched considerably as the concentration of the Cu(II) complex is increased (Figure 2B).
- 3) The formal potential (E°) of the complex experiences a positive shift upon binding to FS-DNA. Furthermore, the voltammetric currents decrease significantly (Figure 2C).
- 4) DPV of the complex experiences a positive potential shift in the cathodic peak potential, along with a significant decrease in the current intensity (Figure 2D).
- 5) Gel retardation assay shows that the migration of the DNA sample has been gradually retarded as the concentration of the Cu(II) complex is increased (Figure 2E).

In addition, using the experimental data and previously reported equations (such as Stern–Volmer equation), the DNA interaction of $[\text{Cu}(\text{tptz})_2](\text{NO}_3)_2$ complex was quantified. The intrinsic binding constant (K_b), Stern–Volmer quenching constant (K_{sv}), and apparent binding constant (K_{app}) for the DNA-Cu(II) interaction were calculated which are $1.5 \times 10^4 \text{ M}^{-1}$, $7.2 \times 10^4 \text{ M}^{-1}$, and $1.1 \times 10^6 \text{ M}^{-1}$, respectively. These results reveal that the complex binds to DNA in a moderately strong fashion.

The chemical nuclease activity of the $[\text{Cu}(\text{tptz})_2](\text{NO}_3)_2$ complex was studied using the supercoiled pEGFP-N1 plasmid in the absence and presence of external agents. As shown in Figure 3 (Lanes 1–8), with increasing concentrations of the $[\text{Cu}(\text{tptz})_2](\text{NO}_3)_2$ complex, SC DNA is gradually converted to NC DNA, revealing the high nuclease activity of the complex. The mechanistic study of the DNA cleavage in the presence of various radical

scavengers (Figure 3; Lanes 9–14) indicates that the complex probably cleaves the DNA strands *via* an oxidative mechanism and the ROSs responsible for the DNA cleavage are likely $^1\text{O}_2$ and O_2^- . Furthermore, it is evaluated that H_2O_2 remarkable catalyzes the nuclease activity of the complex.

An *in-vitro* cytotoxicity study of the complex on MCF-7 cell line by an MTT assay indicates that the $[\text{Cu}(\text{tpzt})_2](\text{NO}_3)_2$ complex exhibits a marked cell growth-inhibitory effect in a dose-dependent manner after 24 h incubation ($\text{IC}_{50} = 1.98 \mu\text{M}$), which is significantly better than that observed for *cis*-platin ($\text{IC}_{50} = 57.9 \mu\text{M}$).

DAPI-staining shows that the majority of the MCF-7 cells treated with the $[\text{Cu}(\text{tpzt})_2](\text{NO}_3)_2$ complex undergoes a considerable chromatin condensation after 16 h, compared to the untreated cells. The morphological changes demonstrate that the Cu(II) complex could inhibit cell proliferation by inducing apoptosis in the breast cancer cells.

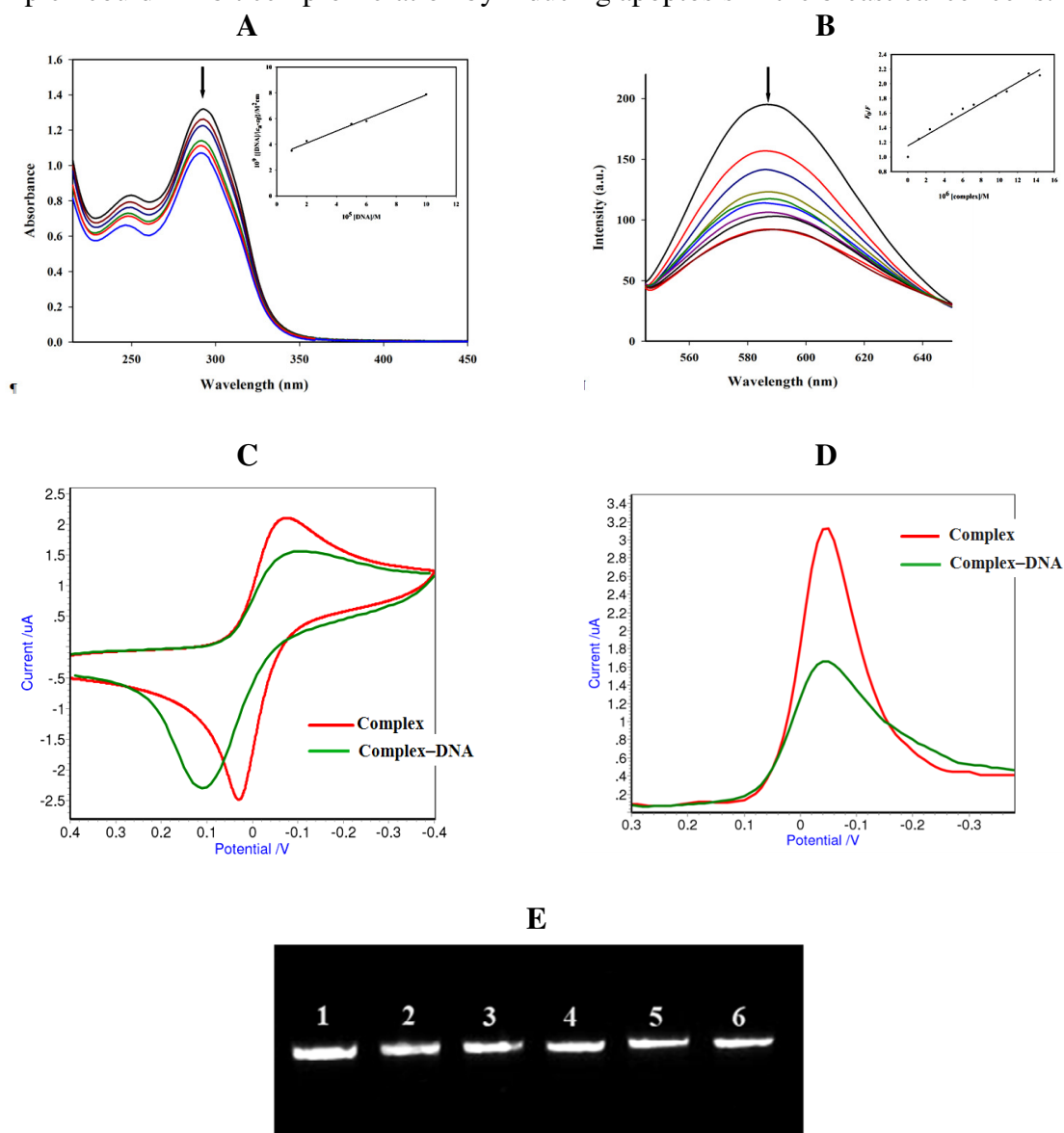


Figure 2. DNA binding studies of the $[\text{Cu}(\text{tpzt})_2](\text{NO}_3)_2$ complex. (A) Changes in the UV spectrum of the Cu(II) complex with increasing concentrations of FS-DNA; (B) Changes in the fluorescence spectrum of "EthBr-DNA" system with increasing concentrations of the Cu(II) complex; (C) Cyclic voltammograms of the Cu(II) complex in the absence and presence of FS-DNA; (D) Differential pulse voltammograms of the Cu(II) complex in the absence and presence of FS-DNA; (E) Changes in the gel electrophoretic mobility of a DNA sample with increasing concentrations of the Cu(II) complex.

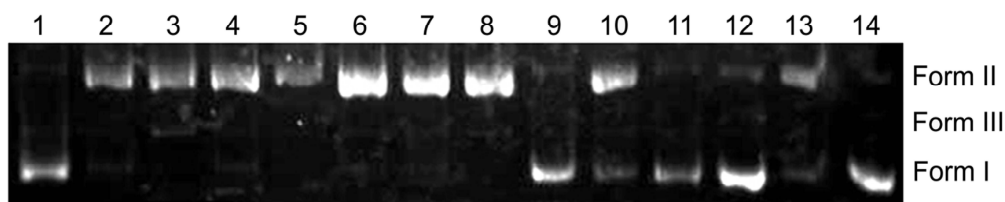


Figure 3. DNA cleavage of the $[\text{Cu}(\text{tptz})_2](\text{NO}_3)_2$ complex at different concentrations. Diagrams show the cleavage of pEGFP-N1 DNA ($0.1 \mu\text{g}/\mu\text{L}$) at different concentrations of the complex in Tris-HCl/NaCl buffer ($\text{pH} = 7.2$) at 37°C for 3 h in the absence and presence of standard radical scavengers. (A) Lane 1: DNA control; Lane 2: DNA + complex ($5 \mu\text{M}$); Lane 3: DNA + complex ($10 \mu\text{M}$); Lane 4: DNA + complex ($30 \mu\text{M}$); Lane 5: DNA + complex ($60 \mu\text{M}$); Lane 6: DNA + complex ($80 \mu\text{M}$); Lane 7: DNA + complex ($100 \mu\text{M}$); Lane 8: DNA + complex ($200 \mu\text{M}$); Lane 9: DNA + complex ($100 \mu\text{M}$) + NaN_3 ($400 \mu\text{M}$); Lane 10: DNA + complex ($100 \mu\text{M}$) + DMSO ($400 \mu\text{M}$); Lane 11: DNA + complex ($100 \mu\text{M}$) + SOD (15 U); Lane 12: DNA + complex ($200 \mu\text{M}$) + NaN_3 ($400 \mu\text{M}$); Lane 13: DNA + complex ($200 \mu\text{M}$) + DMSO ($400 \mu\text{M}$); Lane 14: DNA + complex ($200 \mu\text{M}$) + SOD (15 U).

The $[\text{Cu}(\text{tptz})(\text{dppz})](\text{PF}_6)_2$ complex

The $[\text{Cu}(\text{tptz})(\text{dppz})](\text{PF}_6)_2$ complex was prepared in good yield by the condensation of the $[\text{Cu}(\text{tptz})(\text{phen-dione})](\text{PF}_6)_2$ complex with 1,2-diaminobenzene (2:3 molar ratio) in an acetonitrile solution in the presence of glacial acetic acid. The Cu(II) complex shows two $d \rightarrow d$ transitions at 678 and 958 nm. These LF transitions appear at nearly the same energies to those reported for the $[\text{Cu}(\text{tpy})(\text{NCS})_2]$ complex and indicate that the geometry about the Cu(II) in $[\text{Cu}(\text{tptz})(\text{dppz})](\text{PF}_6)_2$ is very probably of “reverse” C_{2v} -symmetry (or “reverse” square-pyramidal structure).

The DNA interaction studies of the $[\text{Cu}(\text{tptz})(\text{dppz})](\text{NO}_3)_2$ complex suggest that this complex binds to CT-DNA through an intercalative mode involving insertion of the aromatic chromophore of the dppz ligand between the base pairs of ds-DNA. This suggestion is based on the following experimental observations:

- 1) A pronounced hypochromism (25%) along with an obvious bathochromic shift (2–3 nm) in the electronic absorptions of the dppz ligand upon the addition of DNA (Figure 4A).
- 2) The fluorescence intensity of the $\Delta\text{-}[\text{Ru}(\text{phen})_2(\text{dppz})]^{2+}$ complex bound to DNA is considerably quenched on the addition of the Cu(II) complex (Figure 4B), indicating the replacement of the intercalated $\Delta\text{-}[\text{Ru}(\text{phen})_2(\text{dppz})]^{2+}$ cations from ds-DNA into an aqueous environment by the Cu(II) complex cations.
- 3) A significant decrease in the molar ellipticity values of both the positive and negative bands of the CD spectrum of CT-DNA, along with some shift in their positions as the concentration of the complex is increased (Figure 4C).
- 4) Negative LD signals for the intra-ligand dppz bands around 375 nm which clearly supports that the plane of the dppz ligand is located perpendicular to the DNA helix axis through the adduct between the Cu(II) complex and DNA. On the other hand, the Cu(II) complex binds to DNA by intercalation of the dppz ligand between the DNA base pairs (Figure 4D).

Furthermore, using the fluorescence quenching data the K_{sv} and K_{app} parameters were calculated for the interaction of the Cu(II) complex with DNA which are $5.7 \times 10^5 \text{ M}^{-1}$ and $9.3 \times 10^6 \text{ M}^{-1}$, respectively. These parameters demonstrate that the $[\text{Cu}(\text{tptz})(\text{dppz})](\text{NO}_3)_2$ complex is an avid metallointercalator to DNA.

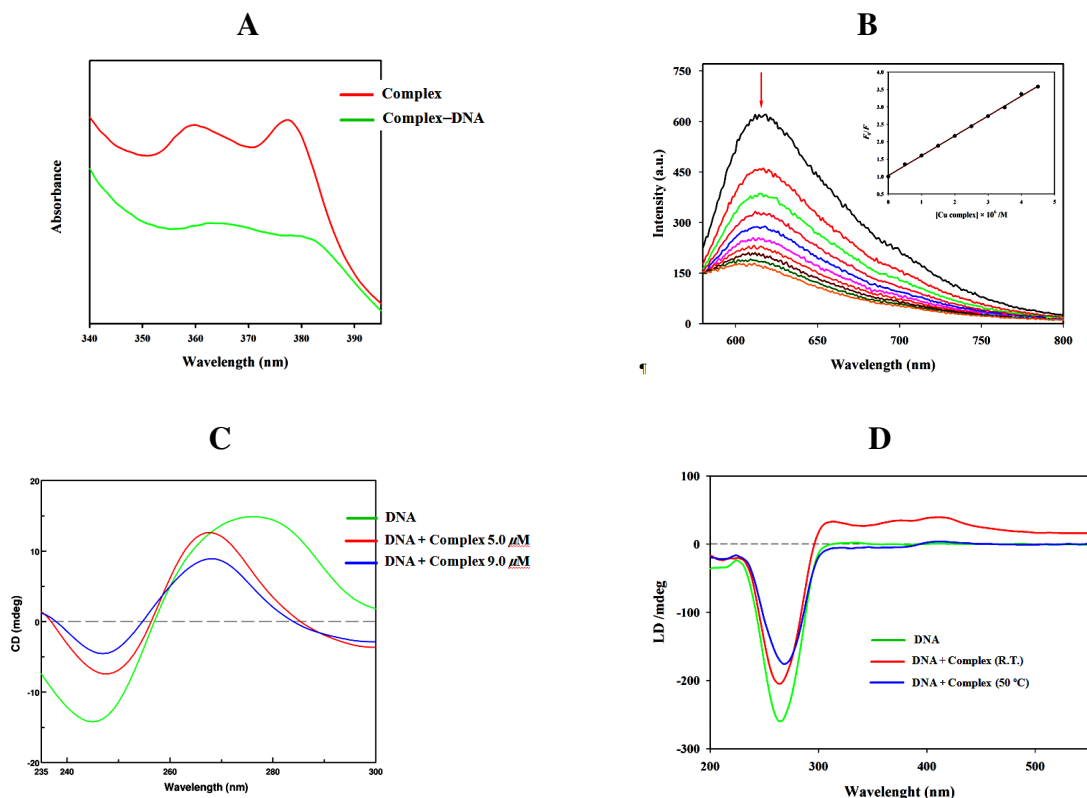


Figure 4. DNA binding studies of the $[\text{Cu}(\text{tpzt})(\text{dppz})](\text{NO}_3)_2$ complex. **(A)** Absorption spectra of the Cu(II) complex in the absence and presence of CT-DNA; **(B)** Changes in the fluorescence spectrum of “ Δ - $[\text{Ru}(\text{phen})_2(\text{dppz})]^{2+}$ -DNA” system with increasing concentrations of the Cu(II) complex; **(C)** Circular dichroism spectra of CT-DNA (smoothed) in the absence and presence of the increasing amounts of the Cu(II) complex; **(D)** Flow linear dichroism spectra of free CT-DNA and upon binding to the Cu(II) complex.

The $[\text{Cu}(\text{tpy})(\text{dppz})](\text{PF}_6)_2$ complex

The $[\text{Cu}(\text{tpy})(\text{dppz})](\text{PF}_6)_2$ complex was prepared *via* a route similar to the tptz analogous complex (i.e. $[\text{Cu}(\text{tptz})(\text{dppz})](\text{PF}_6)_2$). The crystal structure of the complex consists of a discrete monomeric copper(II) species situated on a twofold rotation axis (Figure 5), together with two hexafluorophosphate anions. Interestingly, the Addison's model is not reliable to predict the geometry around the copper atom in this complex and in spite of $\tau = 0.32$, the coordination polyhedron around the copper atom is best described as distorted trigonal-bipyramidal.

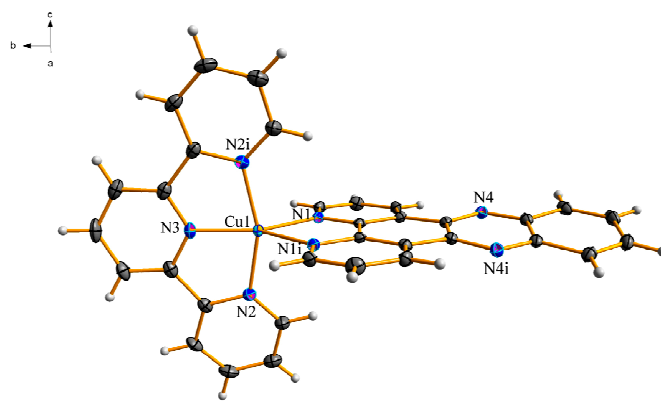


Figure 5. ORTEP view of the molecular structure of $[\text{Cu}(\text{tpy})(\text{dppz})](\text{PF}_6)_2$.

The results of DNA binding studies (Figures 6 A–D) reveal that the $[\text{Cu}(\text{tpy})(\text{dppz})](\text{ClO}_4)_2$ complex binds to CT-DNA through an intercalative mode involving insertion of the aromatic chromophore of the dppz ligand between the base pairs of ds-DNA (in a similar manner to the $[\text{Cu}(\text{tpz})(\text{dppz})](\text{NO}_3)_2$ complex).

The chemical nuclease activity of the $[\text{Cu}(\text{tpy})(\text{dppz})](\text{ClO}_4)_2$ complex was also studied. The results demonstrate that this complex can cleave DNA in a good efficiency. The mechanistic studies reveal that this complex cleaves DNA in a similar manner to the $[\text{Cu}(\text{tpz})_2](\text{NO}_3)_2$. Additionally, H_2O_2 acts an activator for the nuclease activity of this complex.

The capability of the $[\text{Cu}(\text{tpy})(\text{dppz})](\text{ClO}_4)_2$ complex to arrest the proliferation of the MCF-7 cell line was also evaluated by MTT assay after 24 h incubation. It was found that the complex exhibits cytotoxic activity in a concentration-dependent manner with an IC_{50} value of $4.57 \mu\text{M}$. Based on the DAPI staining results it suggests that this complex probably induces the MCF-7 cells to undergo apoptosis.

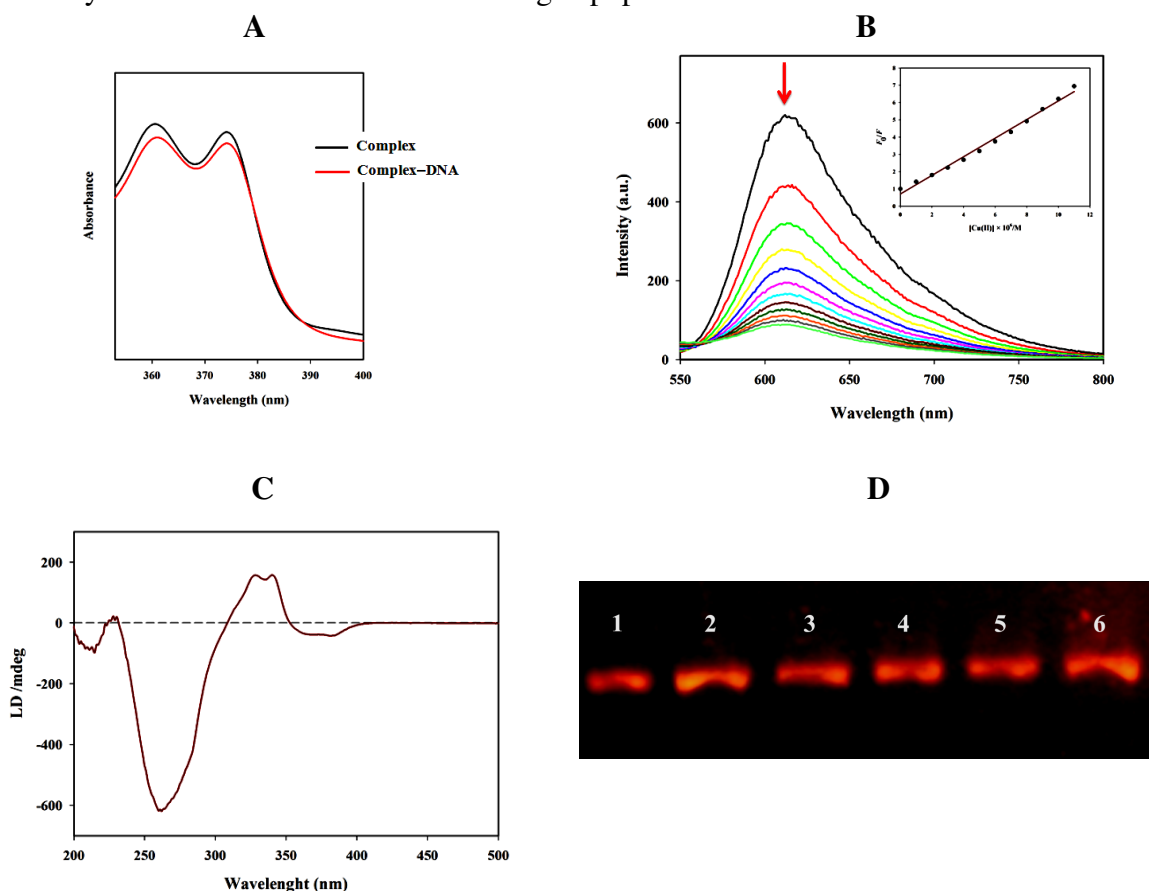


Figure 6. DNA binding studies of the $[\text{Cu}(\text{tpy})(\text{dppz})](\text{ClO}_4)_2$ complex. (A) Absorption spectra of the Cu(II) complex in the absence and presence of CT-DNA; (B) Changes in the fluorescence spectrum of “ Δ - $[\text{Ru}(\text{phen})_2(\text{dppz})]^{2+}$ -DNA” system with increasing concentrations of the Cu(II) complex; (C) Flow linear dichroism spectrum of the $[\text{Cu}(\text{tpy})(\text{dppz})](\text{ClO}_4)_2$ complex bound to CT-DNA; (D) Changes in the gel electrophoretic mobility of a DNA sample with increasing concentrations of the Cu(II) complex.

The $[\{\text{Cu}(\text{tppz})\text{Cl}\}_2(\mu\text{-Cl})](\text{PF}_6)_3$ -toluene complex

Reaction of $\text{CuCl}_2 \cdot 2\text{H}_2\text{O}$, tppz, and AgPF_6 in a stoichiometric ratio of 2:2:1 at room temperature gives the $[\{\text{Cu}(\text{tppz})\text{Cl}\}_2(\mu\text{-Cl})](\text{PF}_6)_3$ complex in a high yield and purity. The crystal structure of the complex consists of a discrete dinuclear copper(II) species (Figure 7), together with a hexafluorophosphate counteranion and a toluene solvent molecule. In this complex, the tppz ligands function as a mono-tridentate ligand.

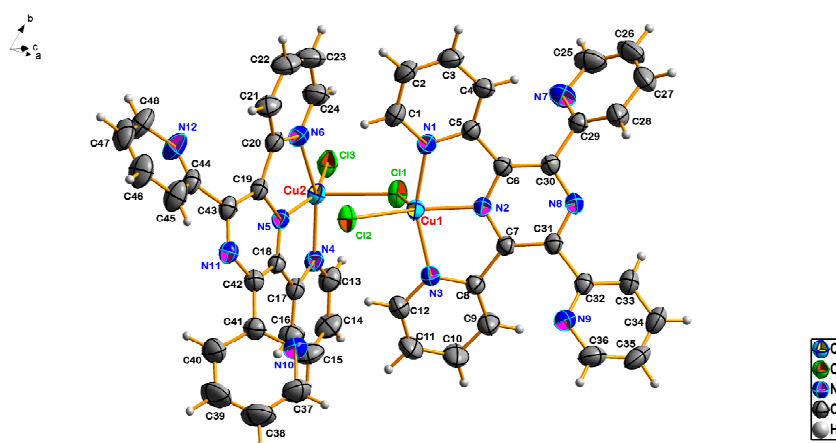


Figure 7. ORTEP view of the molecular structure of $[\{Cu(tppz)Cl\}_2(\mu-Cl)](PF_6) \cdot \text{toluene}$.

The interaction of the $[\{Cu(tppz)Cl\}_2(\mu-Cl)](NO_3)$ complex with FS-DNA has been studied by electronic absorption (Figure 8A) and fluorescence (Figure 8B) titration. The complex emits luminescence in a buffer when excited at 303 nm. The emission intensity of complex is gradually enhanced as the concentration of DNA is increased. The increase in the emission intensity reveals that the interaction between the complex and DNA results in the inaccessibility of the solvent water molecules, thus the collision between the water molecules (quenchers) and the complex decreases. The data of electronic absorption titration were fitted in the McGhee–von Hippel equation (inset of Figure 8A) and the binding constant (K_b) and binding site size (s) were calculated which are $7.4 \times 10^3 \text{ M}^{-1}$ and 0.72, respectively. These parameters demonstrate that this complex moderately binds to DNA *via* partial intercalation and/or groove binding.

The interaction of the $[\{Cu(tppz)Cl\}_2(\mu-Cl)](NO_3)$ complex with BSA has been also studied by fluorescence and electronic absorption titration. The fluorescence intensity of BSA at 346 nm, gradually quenched in the presence of increasing concentrations of the complex (Figure 9A). Furthermore, by increasing the concentration of Cu(II) complex, the intensity of the absorption peak of BSA at 228 nm decreased, and the peak shifted slightly toward longer wavelength, whereas the intensity of BSA peak at 278 nm increased (Figure 9B). These observations reveal the change in the microenvironment around BSA with the

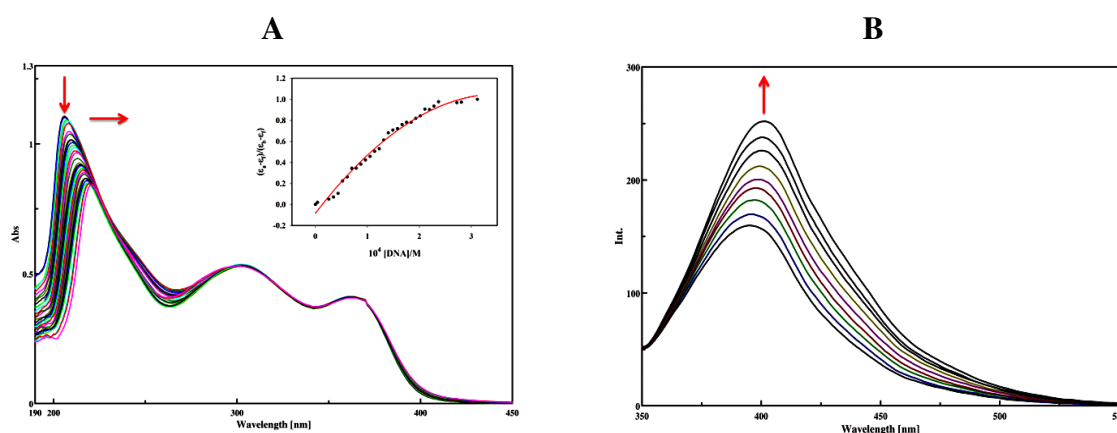


Figure 8. DNA binding studies of the $[\{Cu(tppz)Cl\}_2(\mu-Cl)](NO_3)$ complex. (A) Changes in the UV spectrum of the Cu(II) complex with increasing concentrations of FS-DNA; (B) Changes in the fluorescence spectrum of the Cu(II) complex with increasing concentrations of FS-DNA.

addition of the complex. Using the fluorescence titration data and previously reported equation, the interaction of complex with BSA was quantified (inset of Figure 9A). The binding constant (K_b) and the number of binding sites per albumin molecule (n) for the BSA-Cu(II) interaction were calculated which are $2.3 \times 10^5 \text{ M}^{-1}$ and 0.92, respectively. These results reveal a moderate binding affinity between the Cu(II) complex and BSA with a molar ratio of 1:1. Additionally, the Förster resonance energy transfer (FRET) theory was used to determine the distance (r) between the amino acid residues on the BSA and the Cu(II) complex in the binding site. According to the previously reported equations and the experimental data, the $r = 3.65 \text{ nm}$ was calculated for the Cu(II) complex-BSA interaction.

The chemical cleavage of DNA as a consequence of increasing the concentration of the Cu(II) complex in the presence of ascorbic acid (as an activator) shows the conversion of the supercoiled form into the nicked circular form and even to the linear form, indicating the involvement of the complex in a single and double strand DNA cleavage. No such a DNA cleavage was observed when the ascorbic acid is absent, demonstrating an oxidative mechanism for the nuclease activity of this complex.

The capability of the $[\{\text{Cu}(\text{tppz})\text{Cl}\}_2(\mu\text{-Cl})](\text{NO}_3)$ complex to arrest the proliferation of the MCF-7 cell line was also evaluated by MTT assay after incubation times of 24, 48, and 72 h. It was found that the complex exhibits cytotoxic activity in a concentration-dependent manner with the IC_{50} values of $> 50 \mu\text{M}$ for 24 h, $18.52 \mu\text{M}$ for 48 h, and $16.03 \mu\text{M}$ for 72 h. These results show that the $[\{\text{Cu}(\text{tppz})\text{Cl}\}_2(\mu\text{-Cl})](\text{NO}_3)$ complex has a lower cytotoxic effect on the MCF-7 compared to the $[\text{Cu}(\text{tptz})_2](\text{NO}_3)_2$ and $[\text{Cu}(\text{tpy})(\text{dppz})](\text{ClO}_4)_2$ complexes which is in agreement with their DNA-binding affinities and nuclease activities.

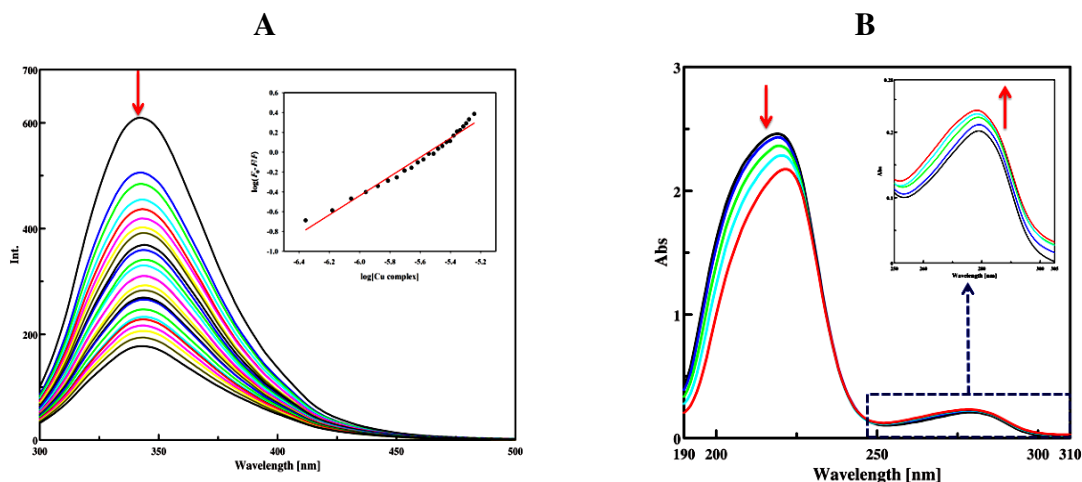


Figure 9. BSA binding studies of the $[\{\text{Cu}(\text{tppz})\text{Cl}\}_2(\mu\text{-Cl})](\text{NO}_3)$ complex. (A) Changes in the fluorescence spectrum of BSA with increasing concentrations of the Cu(II) complex (Inset: Determination of the Cu(II) complex-BSA binding constant and the number of binding sites on BSA); (B) Changes in the UV spectrum of BSA with increasing concentrations of the Cu(II) complex.

The $[\text{Cu}_2(\mu\text{-Cl})_2(\mu\text{-tppz})]_n(\text{PF}_6)_{2n}$ complex

The $[\text{Cu}_2(\mu\text{-Cl})_2(\mu\text{-tppz})]_n(\text{PF}_6)_{2n}$ complex was prepared in high yield and purity by refluxing a mixture of $\text{CuCl}_2 \cdot 2\text{H}_2\text{O}$, tppz, and AgPF_6 (2:1:2) in DMF. The crystal structure of this complex is characterized by a one-dimensional polymeric chain in which both the tppz and chloro ligands function as bridging ligands (Figure 10). The CuN_3Cl_2 coordination sphere of Cu(II) is best described as distorted square-pyramidal ($\tau = 0.269$). Interestingly, the PF_6^- counteranions are arranged besides the cationic chain of the polymer via semi-coordination interactions of $\text{Cu} \cdots \text{F}$ (2.579 \AA).

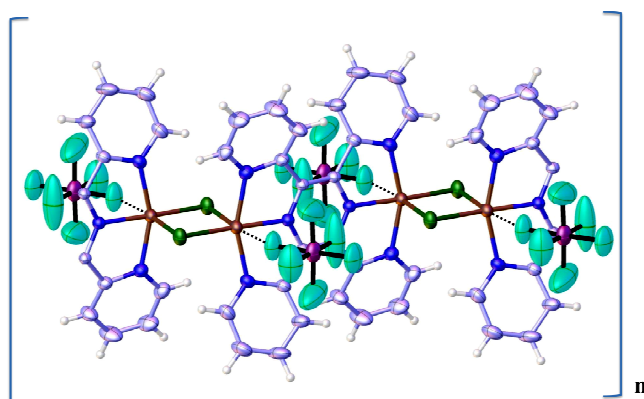


Figure 10. ORTEP view of the molecular structure of $[\text{Cu}_2(\mu\text{-Cl})_2(\mu\text{-tpz})]_n(\text{PF}_6)_{2n}$.

Conclusion

In this thesis, several polypyridyl complexes of Cu(II) were designed, synthesized and characterized. Several biological activities of these complexes such as DNA binding, BSA binding, DNA cleavage, cytotoxicity, and apoptotic activity were investigated. It revealed that some structural and electronic parameters such as the planarity, the hydrophobicity, and the π system area of the ligand, along with the coordination polyhedron and the charge of the complex can affect the DNA binding mode and propensity of the complex. So that the $[\text{Cu}(\text{tpz})(\text{dppz})](\text{NO}_3)_2$ and $[\text{Cu}(\text{tpy})(\text{dppz})](\text{ClO}_4)_2$ complexes are avid metalointercalators to DNA due to the presence of the dppz ligand with an extended π system, while the two complexes $[\text{Cu}(\text{tpz})_2](\text{NO}_3)_2$ and $[\{\text{Cu}(\text{tpz})\text{Cl}\}_2(\mu\text{-Cl})](\text{NO}_3)$ containing the tpz and tpz ligand with pendant pyridyl rings, bind to DNA *via* partial intercalation and/or groove binding. An *in-vitro* cytotoxicity study of the complexes on MCF-7 cell line by MTT assay after 24 h incubation gives an order: $[\text{Cu}(\text{tpz})_2](\text{NO}_3)_2$ ($\text{IC}_{50} = 1.98 \mu\text{M}$) > $[\text{Cu}(\text{tpy})(\text{dppz})](\text{ClO}_4)_2$ ($\text{IC}_{50} = 4.57 \mu\text{M}$) > $[\{\text{Cu}(\text{tpz})\text{Cl}\}_2(\mu\text{-Cl})](\text{NO}_3)$ ($\text{IC}_{50} > 50 \mu\text{M}$). These results indicate that the complexes display good or even excellent cytotoxic effect on MCF-7 cells which are significantly better than that observed for *cis*-platin ($\text{IC}_{50} = 57.90 \mu\text{M}$) under the same conditions. Furthermore, the cytotoxic activity of the complexes is in agreement with their chemical nuclease activity with an order: $[\text{Cu}(\text{tpz})_2](\text{NO}_3)_2$ > $[\text{Cu}(\text{tpy})(\text{dppz})](\text{ClO}_4)_2$ > $[\{\text{Cu}(\text{tpz})\text{Cl}\}_2(\mu\text{-Cl})](\text{NO}_3)$. Consequently, we suggest that the probable mechanism involved in the anti-breast cancer activity of these complexes is the DNA cleavage mechanism.

The results of this thesis, although preliminary, are promising and may shed some light on designing new potential anticancer agents in the future.

Acknowledgement

We are grateful to the Isfahan University of Technology (IUT) for financial support.

References

Barve, A., Kumbhar, A., Bhat, M., Joshi, B., Butcher, R., Sonawane, U., Joshi, R., "Mixed-ligand copper(II) maltolate complexes: synthesis, characterization, DNA binding and cleavage, and cytotoxicity", *Inorganic Chemistry*, Vol. 48, pp. 9120–9132, 2009.

Chauhan, M., Banerjee, K., Arjmand, F., "DNA binding studies of novel copper(II)

- complexes containing *L*-tryptophan as chiral auxiliary: in vitro antitumor activity of Cu-Sn₂ complex in human neuroblastoma cells", *Inorganic Chemistry*, Vol. 46, pp. 3072–3082, 2007.
- Chen, G.-J., Qiao, X., Qiao, P.-Q., Xu, G.-J., Xu, J.-Y., Tian, J.-L., Gu, W., Liu, X., Yan, S.-P., "Synthesis, DNA binding, photo-induced DNA cleavage, cytotoxicity and apoptosis studies of copper(II) complexes", *Journal of Inorganic Biochemistry*, Vol. 105, pp. 119–126, 2011.
- Chen, Q.-Y., Fu, H.-J., Huang, J., Zhang, R.-X., "Synthesis, characterization, bioactivities of copper complexes with N-allyl di(picoly)amine", *Spectrochimica Acta Part A: Molecular and Biomolecular Spectroscopy*, Vol. 75, pp. 355–360, 2010.
- Chen, Q.-Y., Fu, H.-J., Zhu, W.-H., Qi, Y., Ma, Z.-P., Zhao, K.-D., Gao, J., "Interaction with DNA and different effect on the nucleus of cancer cells for copper(II) complexes of N-benzyl di(pyridylmethyl)amine", *Dalton Transactions*, Vol. 40, pp. 4414–4420, 2011.
- Palanichamy, K., Sreejayan, N., Ontko, A.C., "Overcoming cisplatin resistance using gold(III) mimics: Anticancer activity of novel gold(III) polypyridyl complexes", *Journal of Inorganic Biochemistry*, Vol. 106, pp. 32–42, 2012.
- Patel, M.N., Dosi, P.A., Bhatt, B.S., "Nucleic acid interaction and antibacterial behaviours of a ternary palladium(II) complexes", *Spectrochimica Acta Part A: Molecular and Biomolecular Spectroscopy*, Vol. 86, pp. 508–514, 2012.
- Santini, C., Pellei, M., Gandin, V., Porchia, M., Tisato, F., Marzano, C., "Advances in copper complexes as anticancer agents", *Chemical Reviews*, Vol. 114, pp. 815–862, 2013.
- Song, Y.-L., Li, Y.-T., Wu, Z.-Y., "Synthesis, crystal structure, antibacterial assay and DNA binding activity of new binuclear Cu(II) complexes with bridging oxamidate", *Journal of Inorganic Biochemistry*, Vol. 102, pp. 1691–1699, 2008.
- Zhang, C.X., Lippard, S.J., "New metal complexes as potential therapeutics", *Current Opinion in Chemical Biology*, Vol. 7, pp. 481–489, 2003.